International Journal of Research and Innovations in Earth Science
Volume 4, Issue 3, ISSN (Online) : 2394-1375

Modeling Rain Rate Distribution Per Diameter Class from Disdrometer Data Collected in Northern Benin (AMMA Campaign): A New Relationship Between Radar Reflectivity and Rainfall Rate

Kougbéagbédè Hilaire[1], Houngninou B. Etienne[1] and Moumouni Sounmaila[2]
[1]Faculté des Sciences Techniques, Université d'Abomey-Calavi, Bénin
[2]Ecole Normale Supérieure Natitingou, Université de Parakou, Bénin.

***Abstract* — We analyzed the DSD with a new function R(D) which is equal to the rain rate per interval of raindrop diameters. The expressions of some weather variables (radar reflectivity Z, liquid water content W and rainfall rate R_T) were written with the function. The disdrometer data collected in northern of Benin during the African Monsoon Multidisciplinary Analysis (AMMA), were divided into two samples: DATA A and DATA B written in rain rate distribution per diameter class form (R-DSD). The R-DSD of DATA A classified by intervals of rainfall rates are averaged. Gamma function with three parameters (R_T, Dc and μ) models these averaged R-DSD. Various relations are established between the parameters of these averaged R-DSD. Thus, when the moments of these R-DSD are parameterized only by the rain rate R_T, we make a relationship between the radar reflectivity Z and rain rate R_T. Using the sample DATA B allows us to estimate Z by this relation, on one hand, and by the classical Z-R_T relation.**

The comparison of the two estimations allows us to state that the new Z-R_T relation is in the same order as the classical Z-R_T relation.

***Keywords* — DSD, Radar Reflectivity, Rainfall Rate, Disdrometer, AMMA.**

I. Introduction

Most work [1]-[7] which followed that of Marshall and Palmer (1948) [8] on the DSD (Drop Size Distribution) analyze it using a generalized function N(D). It is defined by the spectrum of a given period T (one minute) and corresponds to the number of rain drops per unit of volume and by interval of diameters. It is calculated as follows:

$$N(D_i) = \frac{N_i}{ST\Delta D_i V(D_i)} \quad (1)$$

D_i is the equivalent diameter of the raindrops measured. ΔD_i is the width of the range of diameters centered on D_i. In this study, D_i and ΔD_i are expressed in millimeters. S is the disdrometer collecting area expressed in square meters. At the period T, N_i is the number of drops counted by the disdrometer in each size range. $V(D_i)$ is the falling speed of the drops of diameter D_i. For the rainfall to be proportional to the moment of the function N(D), the relationship between the speed of falling drops and its diameter is used as suggested by Atlas and Ulbrich (1977) [9]:

$$V(D_i) = 3.78 D_i^{0.67} \quad (2)$$

In our study, T is 60 seconds. Therefore, $N(D_i)$ is expressed in $[m^{-3}mm^{-1}]$.

The measured moments of order *n* of the distribution are defined by:

$$M_n = \sum_i D_i^n N(D_i)\Delta D_i \quad (3)$$

When a mathematical function is used to model this distribution, we define the n^{th} theoretical moments as follows:

$$M_n = \int_0^{+\infty} D^n N(D) dD \quad (4)$$

This formula does not account for the truncation of the distribution [10]. However, it has the advantage, for a given function of N(D), to easily write the moments Mn using tabulated mathematical functions.

The function N(D) is commonly used because most application variables in meteorology are written according to those n^{th} statistical moments. These variables are for instance liquid water content, rainfall, the median volume diameter, and radar reflectivity. Moreover, these variables are calculated independently of the inherent form of the DSD. For example, some of their expressions are given below:

- The rain rate $R_T(mm.h^{-1})$: for a given spectrum, the volume of water (converted in height per square meter) measured per unit of time (hour) is given by the following expression:

$$R_T = 6\pi 10^4 \sum_i D_i^3 V(D_i) N(D_i)\Delta D_i \quad (5)$$

Using expression (2), we observe that the rain rate is proportional to the moment of order 3.67.

- The liquid water content $W(g.m^{-3})$: used for the study of microphysical mechanisms of precipitation, the liquid water content is defined as the mass of liquid water in a unit volume of air. By DSD spectrum, the liquid water content is consequently the product of the density of liquid water ($\rho=10^6$ g.m^{-3}) times the sum of the volume of all drops measured in one minute:

$$W = \frac{\pi}{6} 10^{-3} \sum_i D_i^3 N(D_i)\Delta D_i \quad (6)$$

It is, therefore, proportional to the 3^{th} moment of DSD.

- The radar reflectivity in the approximation of Rayleigh $Z(mm^6m^{-3})$: in the particular case where the diameter of the scattering particles is very small

International Journal of Research and Innovations in Earth Science
Volume 4, Issue 3, ISSN (Online) : 2394-1375

compared to the wavelength, the Rayleigh approximation can be used. This approximation is considered valid for rain and frequencies commonly used by operational weather radar (3GHz or 5GHz). Hence, for a given spectrum, the radar reflectivity factor, generally known as radar reflectivity is obtained as followed:

$$Z = \sum_i D_i^6 N(D_i)\Delta D_i \qquad (7)$$

It is, therefore, equal to the 6^{th} moment of DSD.

- The drop energy flux (rate of kinetic energy) E($J.m^{-2}.h^{-1}$) is the variable of greatest interest in erosion studies and this is given by :

$$E = 3\pi 10^{-4} \sum_i D_i^3 [V(D_i)]^3 N(D_i)\Delta D_i \qquad (8)$$

Expression (2) shows that the drop energy flux is proportional to the moment of order 5.01.

In West African regions, the first studies on drops size distribution of rain were conducted by Sauvageot and Lacaux (1995) [11] and were continued by both Nzeukou et *al.* (2004) [12] and Ochou et *al.* (2007) [13]. These distributions had been observed with the impact disdrometer in Abidjan, Boyélé, Dakar and Niamey (Fig.1). Ochou (2003) [14] described the global characteristics of the raindrops size distribution of West African rainfall compared with those of other climatic areas. This work highlighted a remarkable difference between the form of raindrops size distribution of the temperate regions and that of the tropical regions. These authors also analyzed the regional variability of raindrops size distributions within the West African region. They noticed that the moderate rain rates (2 to 20 mm/h) are generated by a large number of raindrops on the coastal sites, whereas on the continental sites, a low number of raindrops is enough to produce the same rain rates. Furthermore, the distributions observed in Niamey (Sahelian zone) are clearly distinguished from those observed in wet tropical zone (Abidjan and Boyélé) based on the relatively higher average size of their drops.

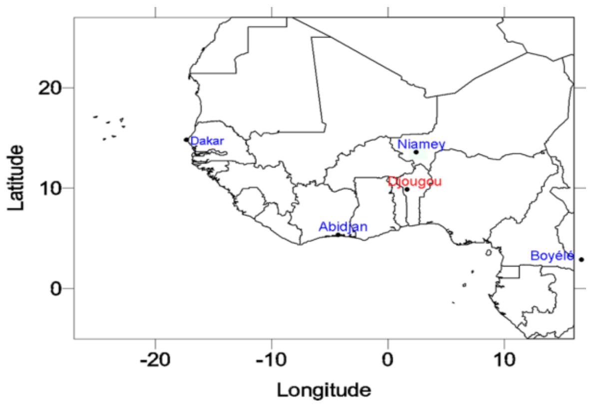

Fig. 1. Region of West Africa with the cities in which DSD was sampled once.

More recently, Moumouni et *al.* (2008) [1] analyzed the drops size distributions collected with optical disdrometers in the same area. They showed that these spectra have a marked convex shape, characteristic of a relative deficit in small drops, as already observed in the area by previous authors. They also indicated that this form of DSD is well reproduced by the gamma function with three parameters and proved that these DSD are very deficient in raindrops number compared to rains in temperate zones.

The objective of this article is methodological. If the quantitative estimation of precipitation is the ultimate goal of weather radars, Why are the variables measured not directly related to the R-DSD, or to their moments? Specifically, we want to verify, using disdrometer data collected from northern Benin, whether the R-DSD can be modeled by the gamma function, and whether the moments of this distribution can be estimated from this model.

II. Data

Optical disdrometers [15-18] belong to the new generation of sensors that measure the size of raindrops. There are currently two types of them: optical disdrometers with only one beam (OSP: Optical Spectro-Pluviometer) and those with double beam (DBS: Dual Beam Spectropluviometer). During the Enhanced Observing Period (EOP) of AMMA campaign [19], these two types of optical disdrometers were used to reinforce the observations of weather radar installed in Djougou, northern of Benin (Figure 1). For technical reasons, these instruments did not work simultaneously.

Table 1 presents the characteristics of the instruments, the geographical coordinates of their installation points and the operating periods. During three rainy seasons (2005 to 2007), these optical disdrometers observed the rain on three sites, in the center and around the city of Djougou. Overall, 93 events were sampled, which represent 11647 spectra of DSD (of duration one minute) and 1221 mm of cumulated rain. The comparison [20] of these measures to those of rain gauges located near the disdrometers showed a real similarity between the event accumulations and intensity distributions.

This study will base all its assessment on this data. For the relevance of the analysis, these data were divided into two samples:

- DATA A consists of 47 events, a total of 6175 R-DSD spectra, used for modeling the distribution;
- DATA B consists of 46 events, a total of 5472 R-DSD spectra, used for the validation of the moments' model.

III. Method

1.1 Expression of Rain Rate Distribution per Diameter Class

Combining relations (1) and (5), the expression of the R-DSD is as followed:

$$R(D_i) = \frac{6\pi 10^{-4} N_i D_i^3}{ST\Delta D_i} \qquad (9)$$

The formula below calculates its measured n^{th} moment:

$$m_n = \sum_i D_i^n R(D_i)\Delta D_i \qquad (10)$$

As in the case of the DSD, when the R-DSD is modeled, its n^{th} theoretical moment is given by the following formula:

$$m_n = \int_0^{+\infty} D^n R(D) dD \quad (11)$$

The expressions of few weather variables that can be deducted from the R-DSD are:

Table 1. Synthesis of the disdrometers data observed in northern Benin. Characteristics of the disdrometers, coordinates of the measuring sites and operating periods of each sensor. IR: Infrared [1].

Sensor name / Type of Disdrometer / Horizontal section	Location / coordinates	Operating period	Number of events/ number of spectra / Total cumulative rainfall
Parsivel / OSP with one beam IR / S=48.6cm^2	Nangatchiori/ 1.74° E, 9.65° N	August to October 2005	10 events / 1816spectra / 160.03mm
DBS-01 / OSP double beam IR / S=100cm^2	Copargo / 1.56° E, 9.82° N	June to september 2006	27 events / 3101spectra / 325.12mm
OSP-01 / OSP double beam IR / S=100cm^2	Djougou / 1.66°E, 9.69°N	June to September 2006	14 events / 1772spectra / 256.10mm
OSP-02 / OSP à simple faisceau IR / S=100cm^2	Djougou / 1.66°E, 9.69°N	June to October 2007	42 events / 4958spectra / 479.65mm

- Rain rate R_T (mm.h^{-1})]: obviously, for a spectrum, rain rate is equal to zeroth moment in this distribution:

$$R_T = \sum_i R(D_i)\Delta D_i \quad (12)$$

- Liquid water content W (g.m^{-3}): by combining relations (5) and (6), for each spectrum, its expression is in the form:

$$W = \frac{10}{36}\sum_i \frac{R(D_i)}{V(D_i)}\Delta D_i \quad (13)$$

Additionally, if we take relation (2) into account, the liquid water content is proportional to the -0.67th moment of the R-DSD.

- Radar reflectivity in the approximation of Rayleigh Z(mm^{6}m^{-3}): its expression is obtained by combining relations with Equations (5) and (7), for each spectrum.

$$Z = \frac{10^4}{6\pi}\sum_i \frac{D_i^3 R(D_i)}{V(D_i)}\Delta D_i \quad (14)$$

Consequently, if we use relation (2), the radar reflectivity in Rayleigh approximation is proportional to the moment of order 2.33 of R-DSD.

- The drop energy flux E(Jm^{-2}h^{-1}) by combining relations (5) and (8), for each spectrum, its expression is in the form:

$$E = 0.5\sum_i [V(D_i)]^2 R(D_i)\Delta D_i \quad (15)$$

Using expression (2) shows that the drop energy flux is proportional to the moment of order 1.34 of R-DSD.

- Characteristic diameter D_c (mm): we also define a diameter which can characterize the average size of the raindrops in a spectrum by the following expression:

$$D_c = \frac{m_1}{m_0} = \frac{\sum_i D_i R(D_i)\Delta D_i}{\sum_i R(D_i)\Delta D_i} \quad (16)$$

1.2 R-DSD Modeling Using a Gamma Function

Given the focus of this article, it is necessary that the R-DSD be modeled by a function with parameter R_T. Consequently, we adopted an analytical expression of the gamma distribution as follows:

$$R(D) = \frac{R_T(\mu+1)^{(\mu+1)}}{D_c\Gamma(\mu+1)}\left(\frac{D}{D_c}\right)^{\mu}\exp\left[-(\mu+1)\frac{D}{D_c}\right] \quad (17)$$

When we introduce relation (17) into (11), the expression of the nth theoretical moment of the distribution is:

$$m_n = \frac{R_T}{\Gamma(\mu+1)}\left(\frac{D_c}{\mu+1}\right)^n \Gamma(\mu+n+1) \quad (18)$$

The zeroth, first and second moments are respectively equal to:

$$m_0 = R_T\,;\ m_1 = R_T D_c\,;\ m_2 = R_T D_c^2 \frac{\mu+2}{\mu+1} \quad (19)$$

By combining these three expressions we obtain:

$$\mu = \frac{m_0 m_2 - 2m_1^2}{m_1^2 - m_0 m_2} \quad (20)$$

IV. Results and Analysis

1.3 Analysis of R-DSD Spectrum by Spectrum

This section is dedicated to the presentation and the analysis of results. From the measured spectra of DATA A, R-DSD is calculated using Eq.(9). Then, Eq. (10) calculates the different moments of the distribution. We directly deduce, for each spectrum, the parameters R_T and D_c. Then we estimate, for each spectrum, the parameter μ

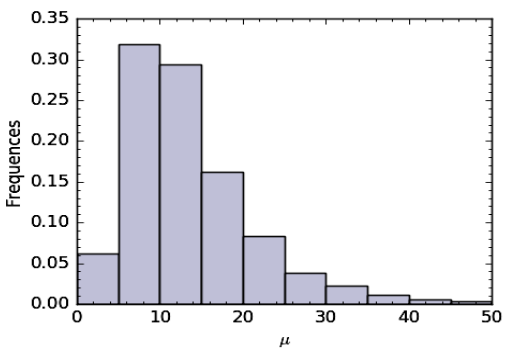

Fig. 2. Histogram of parameter μ values, calculated from 6175 spectra of DATA A.

using the relationship with Eq. (20). Fig.2 displays the histogram of μ values obtained. It reveals that the values of this parameter are strongly dispersed. This result was demonstrated, for the DSD number of drops, by several authors such as Tokay and Short (1996) [21].

This also led other authors [11-13] to calculate and analyze the average of the DSD by class of rain rate. The same situation has led, other authors like Sempere-Torres et *al.* (1994) [22] to suggest a normalization of the DSD with a single parameter, or Testud et *al.* (2001) [23] and Lee et al. (2004) [24] to propose a normalization of the DSD with two parameters. In this work, we adopted the approach of the first authors on the analysis of the averaged R-DSD.

1.4 Analysis of the Average R-DSD

For different classes of rainfall rate of measured spectra DATA A, the average distribution of R-DSD is calculated. Then, the various moments of these average R-DSD helped to determine their R_T, D_c and μ parameters (relationships with Eqs. (19) and (20)). Table 2 reports these values. It also contains the number of spectra for each class. The Nash coefficients and those of correlation calculated between the average R-DSD and the gamma function calibrated on that R-DSD, are also listed in the table. Fig.3 presents the mean R-DSD for different classes of rain intensity. Next, we determined the relationship between these R-DSD parameters (Fig.4).

Based on the analysis of these graphs, it shows that the gamma function fits the R-DSD well. Same as the DSD [1], the R-DSD in northern Benin is convex. The increase in rainfall rate is also justified by the increase in the average size of the raindrops (relation with Eq. (21)). Lastly, the variability of the form parameter μ can be explained by the variability of the rain intensity (relation with Eq. (22)), and therefore by the variability of the characteristic diameter (relation with Eq. (23)).

$$D_c(R_T) = 1.459 R_T^{0.16} \quad (21)$$

$$\mu(R_T) = 4.283 R_T^{0.098} \quad (22)$$

$$\mu(D_c) = 3.354 D_c^{0.628} \quad (23)$$

Table 2. Parameters (R_T, D_c and μ) of gamma function set to the average R-DSD. Coefficients of correlation and Nash calculated between the averaged R-DSD and the model.

Rain rate classes	$R_T \le 5$	$5 \le R_T < 10$	$10 \le R_T < 20$	$20 \le R_T < 30$
Number of spectrum	4589	573	428	228
R_T [mm]	1.442	6.957	14.263	24.249
Dc [mm]	1.740	1.949	2.092	2.310
μ	4.796	4.908	5.837	5.610
ρ	0.993	0.976	0.980	0.984
Nash	0.978	0.933	0.949	0.957
Rain rate classes	$30 \le R_T < 40$	$40 \le R_T < 60$	$60 \le R_T < 100$	$R_T \ge 100$
Number of spectrum	124	122	78	33
R_T [mm]	34.246	48.507	71.999	131.395
Dc [mm]	2.505	2.836	2.884	3.268
μ	5.622	6.273	6.623	7.239
ρ	0.989	0.997	0.997	0.994
Nash	0.971	0.993	0.99	0.985

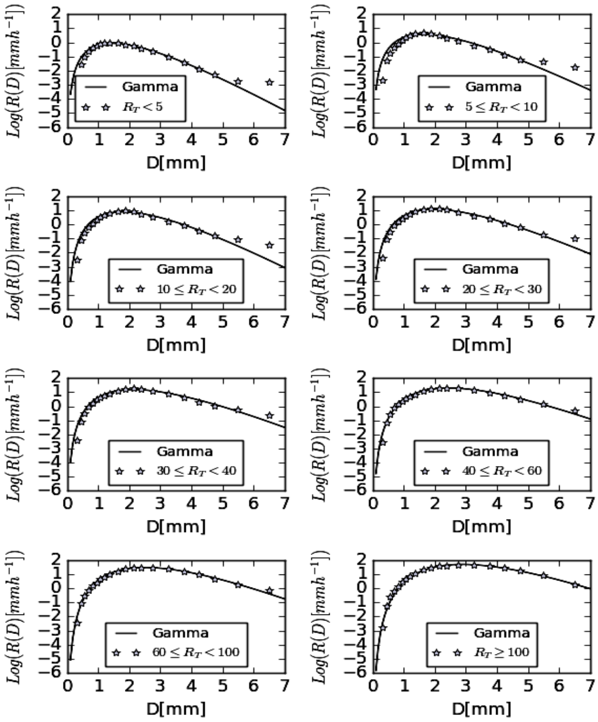

Fig. 3. Spectra of DATA A. Each sample averaged R-DSD class is represented by the symbol and the curve represents the gamma function fitted to this R-DSD.

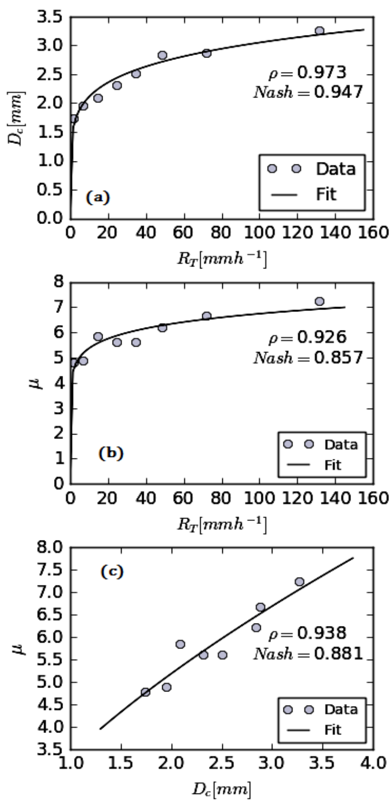

Fig. 4. Spectra of DATA A. Parameters (R_T, D_c and μ) from the averaged R-DSD represented one according to the other (symbol). In each case, the curve represents their relationships adjusted on the data.

1.5 Model Validation

In Section 3, we showed that radar reflectivity Z (in Rayleigh approximation), the liquid water content W and the drop energy flux are respectively proportional to the moments of order 2.33, -0.67 and 1.34 of R-DSD. The rain rate itself being equal to the zeroth moment of R-DSD. Even without the meaning of the other moments, it would be interesting to see how the model can successfully estimate them. Consequently, we compare the measured moments (Eq. (10)) to the theoretical moments (relation with Eq. (18)) using the criteria defined in the annex. The theoretical calculation of moments requires to input three parameters. For this purpose, we adopted the three types of inputs:

Input1: R_T[measured]-D_c[measured]-$\mu(R_T)$[Eq.(22)]
Input2: R_T[measured]-D_c [measured]-$\mu(D_c)$[Eq. (23)]
Input3: R_T[measured]-$D_c(R_T)$[Eq.(21)]-$\mu(R_T)$[Eq. (22)]

Fig.5 displays the results of these comparisons. Apparently, for these three inputs, the theoretical formula on moment estimates precisely the zeroth moment (i.e. the rain intensity). Additionally, the different moments are very well calculated, when we use the first two inputs (Input1 and Input2). This proves the importance of having two parameters to estimate the different moments of the distribution correctly. Concerning the third input (Input3) where we only use the rain intensity as a single input, we notice that the estimation error rapidly increases, when moving away from the zeroth order. However, for orders of moments between -1 and 2, the various criteria show that the estimate is fairly accurate.

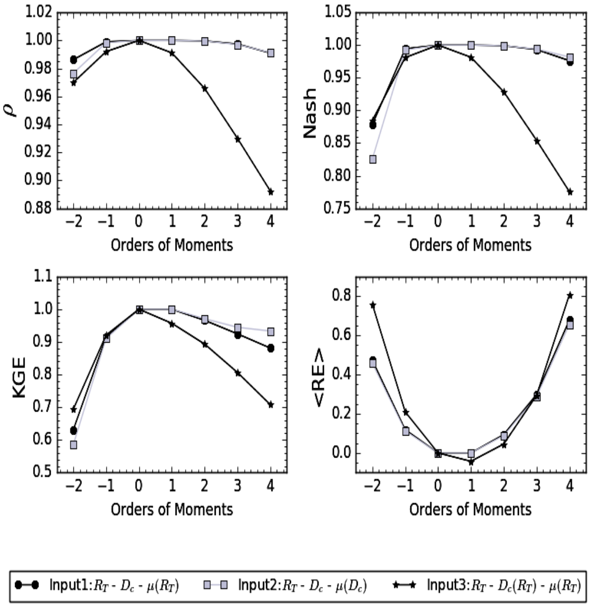

Fig. 5. Spectra of DATA B: Comparison between measured and theoretical moments. Evolution of validation criteria (linear correlation coefficient, Nash coefficient, KGE efficiency and relative error) according to the order moments.

With input 3, the radar reflectivity (in Rayleigh approximation) is as follows:

$$Z = \frac{10^4 R_T}{22.68\pi}\left(\frac{D_c}{\mu+1}\right)^{2.33}\frac{\Gamma(\mu+3.33)}{\Gamma(\mu+1)} \quad (24)$$

With $D_c=D_c(R_T)$ Eq.(21) and $\mu=\mu(R_T)$ Eq. (22).

From the spectra of the sample DATA A, the classical relationship Z-R_T is $Z = 413R_T^{1.33}$.

Using R_T as input, we compared the Z estimation from the Z-R_T relationship to the one from Eq. (24). Fig.6 shows the results. Both estimate are almost in the same order. However, we notice that all the high reflectivity values are underestimated by the classical relation Z-R_T. For the same values, both tendencies (underestimation and overestimation) are observed. Moreover, fig. 6(a) and (b) show that the knowledge of one of the parameters μ or D_c in addition to the radar reflectivity would clearly improve the estimates.

V. Conclusion

Usually, the DSD is analyzed by a N(D) function which is equal to the number of raindrops per unit of volume and raindrops diameter range. In this work, we analyze it using a R(D) function which is equal to the rain rate per interval of diameter. We have established the relationship between this function and each of the following variables: radar reflectivity (in Rayleigh approximation); liquid water content W, rain rate R_T and the drop energy flux E.

Using disdrometer data collected in northern Benin [1], we modeled the R-DSD per intensity range, with a gamma function with three parameters (R_T, D_c and μ). Different relationships have been established between these parameters. The analysis of the relevance of these relations revealed that a good estimation of the moments of the R-DSD requires at least two parameters (R_T and D_c).

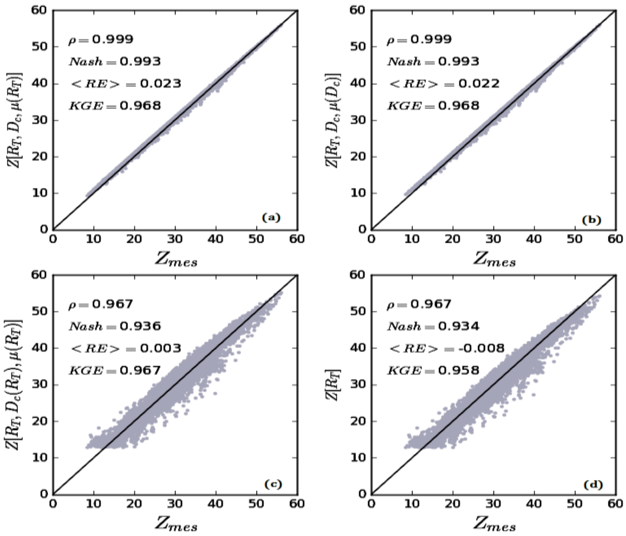

Fig. 6. Spectra of DATA B: Comparison between the measured radar reflectivity Z[dBZ] (x-axis) and those estimated using different approaches. (a) and (b): successively Input 1 and Input 2 the parameters R_T and D_c are used at the entrance. (c): Input 3 or Eq.24. (d): the classic relationship Z-R_T. In both last cases (c and d) only R_T is used at the entrance.

International Journal of Research and Innovations in Earth Science
Volume 4, Issue 3, ISSN (Online) : 2394-1375

When we reduce the number of parameters to only RT, the accuracy of the estimation of the moments is reduced, compared to the case of two parameters (R_T and D_c). However, in that case, the relationship obtained between the radar reflectivity Z and the rain rate R_T is in the same order as the one achieved with the classical relationship Z-R_T. In other way, this study shows that the knowledge of one of the parameters μ or D_c in addition to the radar reflectivity would clearly improve the estimates. In future studies, we will look for possible relationship between these parameters and polarimetric variables.

VI. Annex: Criteria

Let Y^{obs} be an observed data or directly calculated from observations, and Y^{est} be a theoretically estimated data $E[Y^{obs}]$ and $E[Y^{est}]$ their respectively averages, σ_{obs} and σ_{est} their respective standard deviations, the four criteria used to test the efficacy of the model suggested are defined as follows:

The coefficient of linear correlation of Pearson:

$$\rho = \frac{E[(Y^{obs} - E[Y^{obs}])(Y^{est} - E[Y^{est}])]}{\sigma_{obs}\sigma_{est}}$$

The mean relative error: $< R >= E[\frac{(Y^{est} - Y^{obs})}{Y^{obs}}]$

The Nash coefficient [25], defined by:

$$Nash = 1 - \frac{E[(Y^{est} - Y^{obs})^2]}{E[(Y^{obs} - E[Y^{obs}])^2]}$$

The efficiency of Kling-Gupta KGE [26], defined by:

$$KGE = 1 - \sqrt{(\rho - 1)^2 + (\frac{\sigma_{est}}{\sigma_{obs}} - 1)^2 + (\frac{E[Y^{est}]}{E[Y^{obs}]} - 1)^2}$$

References

[1] S. Moumouni; M. Gosset and E. Houngninou, "Main features of rain drop size distributions observed in Benin, West Africa, with optical disdrometers," *Geophys. Res.* Lett. Vol. 35, (L23807) DOI:10.1029/2008GL035755, 2008.

[2] R. Uijlenhoet; M. Steiner and J. A. Smith, "Variability of Raindrop Size Distributions in a Squall line and Implication for Radar Rainfall Estimation," *J. Hydrometeor*, Vol. 4, 2003a, pp. 43-61.

[3] R. Uijlenhoet; J. A. Smith and M. Steiner, "The Microphysical Structure of Extreme Precipitation as Inferred from Ground-Based Raindrop Spectra," *J. Atmos. Sci.*, Vol. 60, 2003b, pp. 1220-1238.

[4] M. Maki; T.D. Keenan; Y. Sasaki and K. Nakamura, "Characteristics of the Raindrop Size Distribution in Tropical Continental Squall Lines Observed in Darwin, Australia," *J. Appl. Meteor*, Vol. 40, 2001, pp. 1393-1412.

[5] D. Atlas; C. W. Ulbrich; F. D. Marks Jr.; E. Amitai and C. R. Williams, "Systematic variation of drop size and radar-rainfall relations," *J. Geophys. Res.* Vol. 104, 1999, pp. 6155-6169.

[6] C. W. Ulbrich and D. Atlas, "Rainfall microphysics and radar properties: Analysis methods for drop size spectra," *J. Appl. Meteor.*, 1998, Vol. 37, pp. 912-923

[7] C. W. Ulbrich, "Natural variation in the analytical form of the raindrop size distribution," *J. Climate Appl. Moteor*., 1983, Vol. 22, pp. 1764-1775.

[8] J.S. Marshall and W. McK. Palmer, "The distribution of raindrop with size," *J. Meteor*., 1948, Vol. 5, pp. 165-166

[9] D. Atlas and C. W. Ulbrich, "Path- and area-integrated rainfall measurement by microwave attenuation in the 1-3 cm band,", *J. App . Meteor.*, 1977 Vol. 16, pp. 1322-1331.

[10] C. W. Ulbrich, "The Effects of Drop Size Distribution Truncation on Rainfall Integral Parameters and Empirical Relations." *J. Climate Appl. Moteor.*, 1985, Vol. 24, pp. 580-590

[11] H. Sauvageot and J. P. Lacaux, "The shape of averaged drop size distributions," *J. Atmos. Sci.*, 1995Vol. 52, pp. 1070-1083.

[12] A. Nzeukou; H. Sauvageot ; A. D. Ochou and C. M. F. Kebe, "Raindrop Size Distribution and Radar Parameters at Cape Verde," *J. Appl. Meteor.*, 2004 Vol. 43, pp. 90-105.

[13] A. D. Ochou; A. Nzeukou and H. Sauvageot, "Parametrization of drop size distribution with rain rate," *Atmos Res.*, 2007, Vol. 84, pp. 58-66

[14] A. D. Ochou, "Variabilité spatio-temporelle des moments statistiques des distributions des gouttes de pluie et conséquences sur la mesure des précipitations par télédétection micro-ondes," *Thèse d'état, Université Cocody-Abidjan*, 2003, pp 138.

[15] E. Campos and I. Zawadzki, "Instrumental Uncertainties in Z-R relations," *J. Appl. Meteor.*, 2000, Vol. 39, pp. 1088-1102.

[16] J.-Y. Delahaye; L. Barthès; P. Golé; J. Lavergnat and J.P. Vinson, "A dual-beam spectropluviometer concept," *J. of Hydrology*, Vol. 328, 2005, pp. 110-120.

[17] M. Löffler-Mang and J. Joss, "An Optical Disdrometer for Measuring Size and Velocity of Hydrometeors," *J. Atmos. Oceanic. Technol.*, Vol. 17, 2000, pp. 130-139

[18] C. Salles; J.D. Creutin and D. Sempere-Torres, "The optical spectropluviometer revisited," *J. Atmos Oceanic. Technol*., vol. 15, 1998, pp. 1215-1222.

[19] J.-L. Redelsperger; C. Thorncroft; A. Diedhiou; T. Lebel; D. Parker and J. Polcher, "African Monsoon, Multidisciplinary Analysis (AMMA): An International Research Project and Field Campaign," *Bull. Amer. Meteorol. Soc.*, Vol. 88, 2006, pp.1739-1746

[20] S. Moumouni, "Analyse des distributions granulométriques des pluies au Bénin : caractéristiques globales, variabilité et application à la mesure radar," *Thèse de Doctorat, INP-Grenoble*, 2009.

[21] A. Tokay and D. A. Short, "Evidence from Tropical Raindrop Spectra of the Origin of Rain from Stratiform versus Convective Clouds," *J. Appl. Meteor*. Vol. 35, 1996, pp. 355-371

[22] D. Sempere-Torres; J. M. Porra and J. D. Creutin, "A general formulation for raindrop size distribution," *J. Appl. Meteorol.*, Vol. 33, 1994, pp. 1494-1502

[23] J. Testud; S. Oury; R. A. Black; P. Amayenc and X. Dou, "The concept of "normalized'' distribution to describe raindrop spectra: A tool for cloud physics and cloud remote sensing," *J. Appl. Meteorol.* Vol. 40, 2001, pp. 1118-1140

[24] G.W. Lee; I. Zawadzki; W. Szyrmer; D. Sempere-Torres and R. Uijlenhoet, "A Genaral Approch to Double-Moment Normalisation of Drop Size Distributions," *J. Appl. Meteor.*, Vol. 43, 2004, pp. 264-281

[25] J. E. Nash and J. V. Sutcliffe, "River flow forecasting through conceptual models part I - A discussion of principles," *J. Hydrol* Vol.10, 1970, pp. 282-290.

[26] H. V. Gupta; H. Kling; K.K. Yilmaz and G.F. Martinez, "Decomposition of the mean squared errorand NSE performance criteria: Implications for improving hydrological modelling."*J. Hydrol*. Vol. 377, 2009, pp. 80-91, doi:10.1016/j.jhydrol.2009.08.003

Acknowledgment

Based on a French initiative, AMMA was built by an international scientific group and is currently funded by a large number of agencies, especially from France, UK, US and Africa. It has been the beneficiary of a major financial contribution from the European Community's Sixth Framework Research Program. Detailed information on scientific coordination and funding is available on the AMMA International web site http://www.amma-international.org.

AUTHORS' PROFILES

Dr. KOUGBEAGBEDE Hilaire
works in Laboratory of Atmospheric Physics , University of Abomey-Calavi, Republic of Benin (West Africa).
Mail: hilairekougbeagbede@gmail.com
Research interest: Meteorological process and Climate Change.

NO PICTURE

Dr. Etienne B. HOUNGNINOU
is a Senior Lecturer in faculty of sciences and technology of University of Abomey-Calavi, Republic of Benin (West Africa).
Mail: houngnb@yahoo.fr
Research interest: Meteorological process and Climate Change;

Dr Sounmaïla MOUMOUNI
is a Senior Lecturer in Higher Teachers' Training School of Natitingou, University of Parakou, Republic of Benin (West Africa).
Research interest: (1) Meteorological process and Climate Change; (2) Theoretical study of diffusion process and its applications.
E-mail:sounma.moumouni@gmail.com
BP 1681 Abomey-Calavi, Republic of Benin